Supporting Information

Surfen-Assembled Graphene Oxide for Fluorescence Turn-On Detection of Sulfated Glycosaminoglycans in Biological Matrix

Yen-Ting Wang[1] and Wei-Lung Tseng*[1,2]

1. Department of Chemistry, National Sun Yat-sen University, Taiwan

2. School of Pharmacy, College of Pharmacy, Kaohsiung Medical University, Taiwan

Correspondence: Dr. Wei-Lung. Tseng, Department of Chemistry, National Sun Yat-sen University, 70, Lien-hai Road, Kaohsiung, Taiwan 804.

E-mail: tsengwl@mail.nsysu.edu.tw

Fax: 011-886-7-3684046.

Abstract

In the section of supporting information, we include detail information associated with the synthesis of FLGO (experimental section), AFM image of FLGO (Figure S1), the scheme for the loading of surfen molecules on the FLGO surface (Figure S2), the chemical structure of surfen and sulfated GAGs (Figures S3 and S14), the effect of the solution pH on the adsorption efficiency of FLGO for surfen (Figure S4), the characterization of surfen-assembled FLGO (Figures S5-S7), the effects of the solution pH, the NaCl concentration, and the plasma concentration on the fluorescence intensity of surfen-assembled FLGO (Figures S8, S9, and S17), a plot of the $(F_0/F - 1)/[Q]$ value against the FLGO concentration (Figure S10), absorption spectra of surfen and surfen-assembled FLGO (Figure S11), fluorescence spectrum of surfen and absorption spectrum of FLGO (Figure S12), fluorescence spectra of surfen-assembled FLGO in the presence of five kinds of sulfated GAGs (Figure S13), the selectivity and sensitivity of surfen toward sulfated GAGs (Figures S15 and S16), surfen-assembled FLGO for the determination of heparin in different kinds of plasma samples (Figure S18), and comparison of surfen-assembled FLGO and the other previously reported methods for sensing heparin in terms of linear range and LOD

(Table S1).

Experimental Section

Synthesis of FLGO. Nature graphite powder was used for the synthesis of FLGO according to Hummer's method. In brief, native graphite flake (1 g) was immersed in a solution of concentrated H_2SO_4 (1.5 mL) consisting of $K_2S_2O_8$ (0.5 g) and P_2O_5 (0.5 g). The resulting solution reacted at 80 °C for 6 h. The obtained product was continuously washed with deionized water until the pH of rinse water was near neutral. After that, the preoxidized graphite (1 g) was mixed with a concentrated H_2SO_4 (23 mL) in a beaker at 0 °C. Subsequently, $KMnO_4$ (3 g) was gradually added to the above solution with continuous stirring while the beaker was kept in the ice bath. After 5 min, the ice bath was removed. The mixture was heated to 35 °C for 2 h with stirring and added to 46 mL of deionized water. After 15 min, the reaction was terminated by adding 140 mL of deionized water (140 mL) and 2.5 mL of 30% H_2O_2; the color of the resulting solution became bright yellow. For the removal of residual metal and SO_4^{2-} ions, the resulting solution was centrifuged at 13000 rpm for 30 min and then washed with 250 mL of 10% HCl. The precipitate was rinsed with deionized water and repeatedly centrifuged until the pH of the rinse water approached to neutral. Exfoliation of the precipitate was performed under the treatment of ultrasound sonication (Elma, South Orange, NJ; 150 W, 135 kHz) for 1 h.

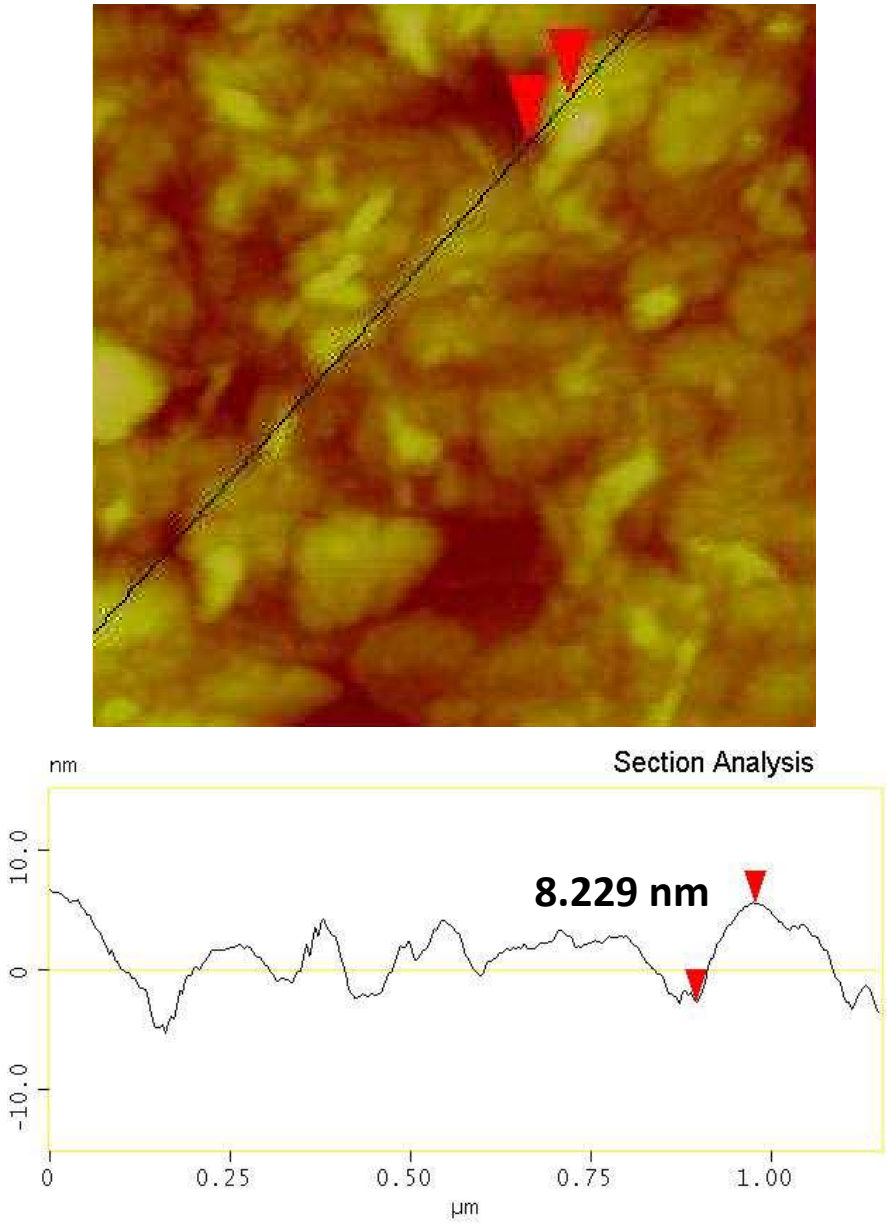

Figure S1. AFM image of FLGO. The height profiles are shown at the bottom.

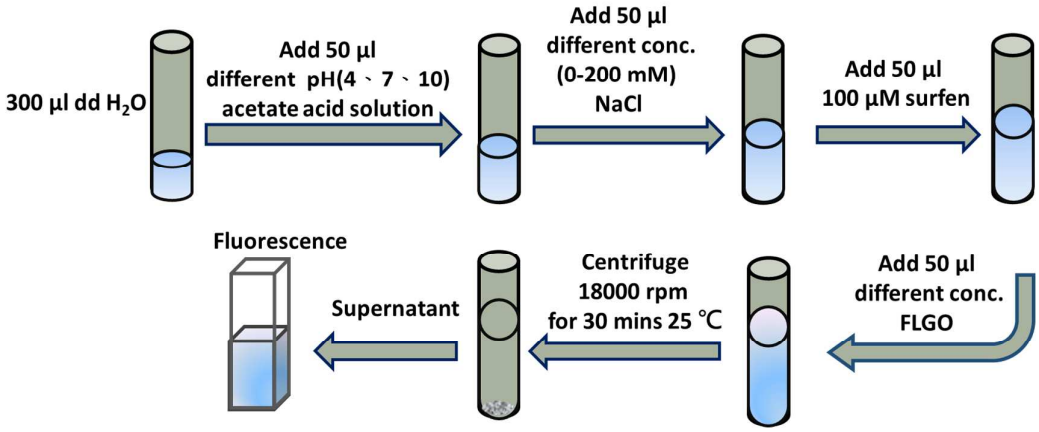

Figure S2. The procedure for the loading of surfen molecules on the surface of FLGO

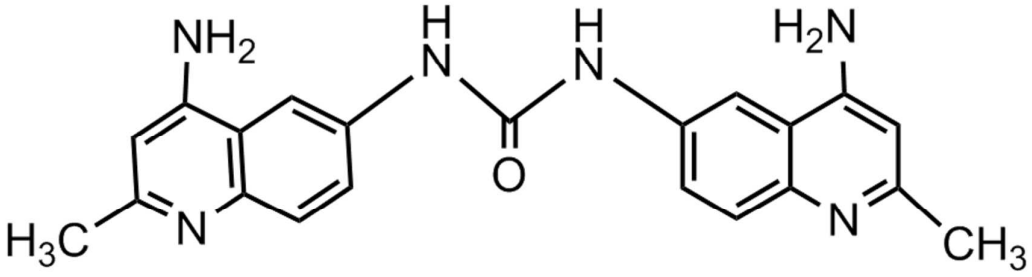

Figure S3. Chemical structure of surfen.

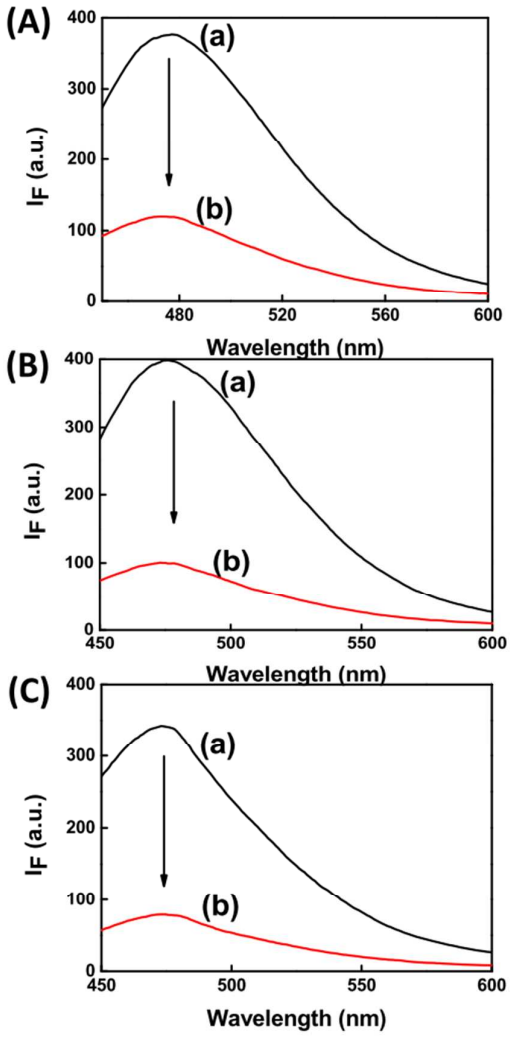

Figure S4. Fluorescence spectra obtained from the incubation of (a) 10 μM surfen and (b) a mixture of 10 μM surfen and 15 μg/mL FLGO under different pH conditions, followed by the centrifugation at 18000 rpm for 30 min: (A) pH 4.0, (B) pH 7.0, and (C) pH 10.0. 15 μg/mL FLGO was incubated with 10 μM surfen at ambient temperature for 10 min at three pH conditions. After the collection of surfen-adsorbed FLGO by centrifugation, the fluorescence intensity of the supernatant corresponding to the unbound surfen was greatly weaker than that of surfen at any pH value. The adsorption efficiencies of surfen on the surface of FLGO at pH 4, 7, and 10 were all determined to be approximately 40%. This result reflects that surfen can be efficiently adsorbed on the surface of FLGO in a wide range of pH.

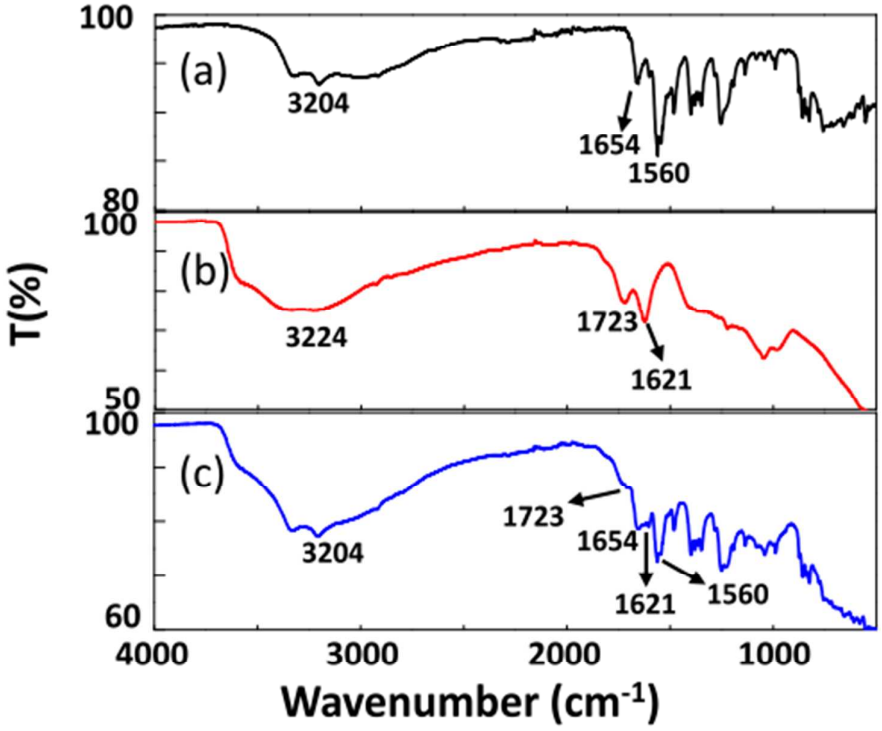

Figure S5. FT-IR spectra of (a) surfen, (b) FLGO, and (c) surfen-assembled FLGO. Surfen was incubated with FLGO in 20 mM sodium acetate (pH 10.0). The concentrations of surfen and FLGO are 10 μM and 15 μg/mL. The FI-IR spectrum of surfen shows several characteristic peaks at 1560, 1654 and 3204 cm^{-1}, which arose from the N-H bending, C=N stretching, and N-H stretching modes, respectively (curve a). The analysis of FLGO by FI-IR shows three strong peaks at 1621, 1723, and 3224 cm^{-1} corresponding to the stretching vibrations of C=C, C=O, and O-H, respectively (curve b). In comparison, the vibrational features of surfen-assembled FLGO resembled the identified functional groups in both FLGO and surfen (curve c).

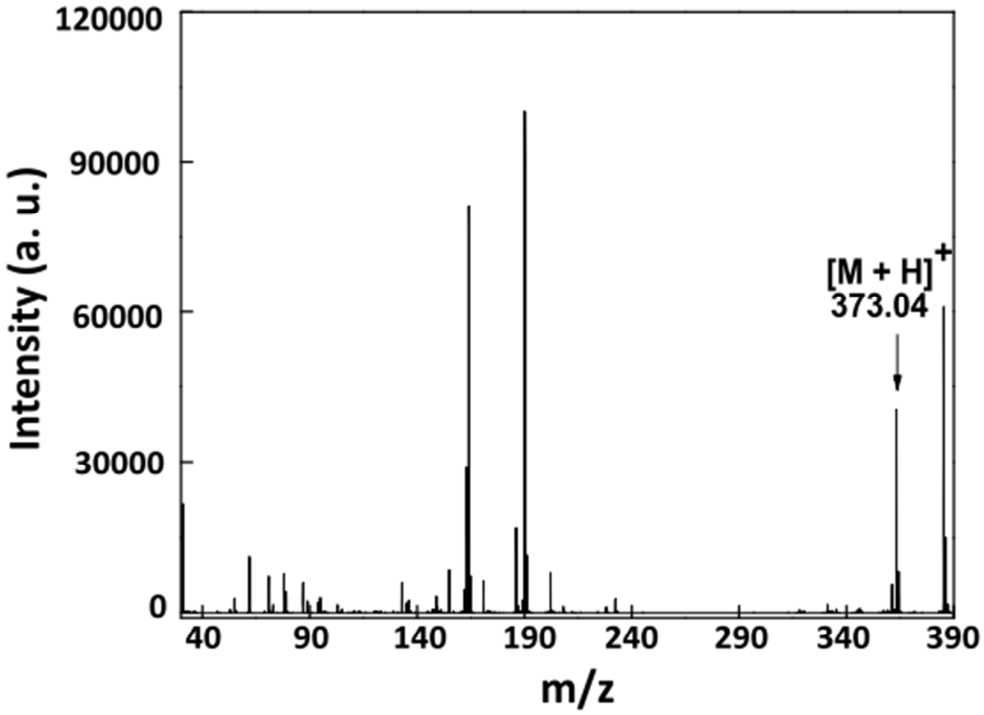

Figure S6. MALDI-TOF mass spectrum of surfen-assembled FLGO. Surfen was incubated with FLGO in 20 mM sodium acetate (pH 10.0). The concentrations of surfen and FLGO are 10 μM and 15 μg/mL. A MALDI-TOF-MS technique was helpful to examine whether or not surfen molecules could attach onto the surface of FLGO. Because FLGO has been reported to be used as a MALDI matrix for the in situ determination of small organic molecules, surfen molecules adsorbed on the surface of FLGO have a much higher opportunity to be ionized by MALDI-TOF-MS than the unbound surfen molecules in bulk solution. The detection of the precipitate by MALDI-TOF MS showed the major peak at *m*/*z* 373.40, which was identified to $[\text{surfen} + \text{H}]^+$.

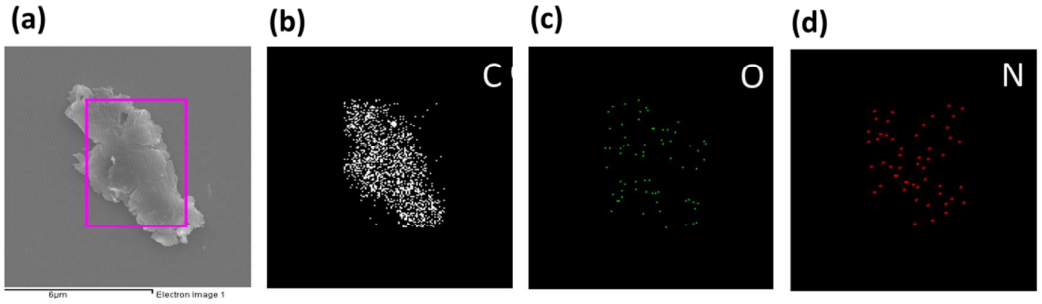

Figure S7. (a) FESEM image of surfen-assembled FLGO. EDS elemental mapping images of (b) C, (c) O, and (d) N elements of surfen-assembled FLGO. The concentrations of surfen and FLGO are 10 μM and 15 μg/mL. The elemental mapping reveals that carbon element was homogeneously distributed in the surfen-assembled FLGO. In addition to carbon elements, oxygen and nitrogen elements were also found in surfen-assembled FLGO. Because FGLO only contains carboxyl and hydroxyl groups, the nitrogen element was suggested to result from surfen.

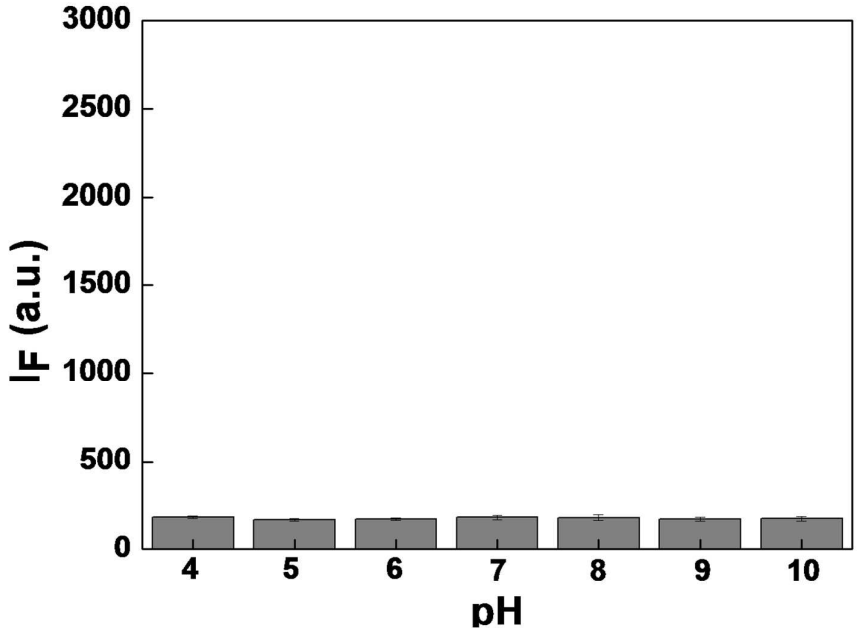

Figure S8. Fluorescence intensity of surfen-assembled FLGO at 485 nm as a function of pH.

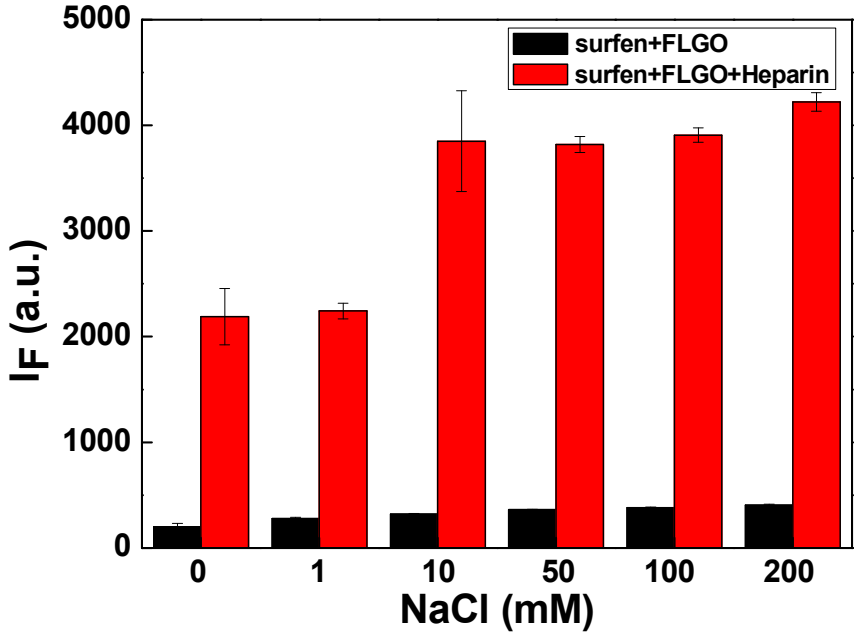

Figure S9. Fluorescence intensity of surfen-assembled FLGO at 485 nm as a function of the concentration of NaCl in the absence (black bar) and presence (red bar) of 100 nM heparin.

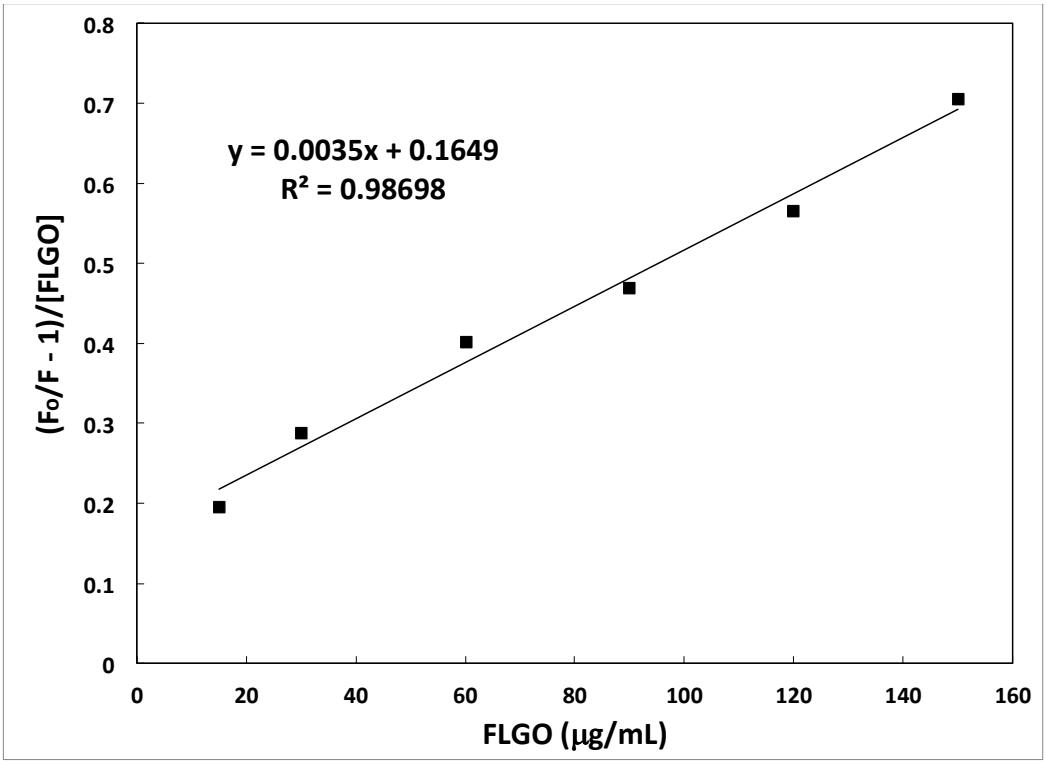

Figure S10. A plot of the value of (F_0/F – 1)/[FLGO] versus the concentration of FLGO. F_0 and F correspond to the fluorescence intensities of surfen at 485 nm before and after the addition of different concentrations of FLGO, respectively.

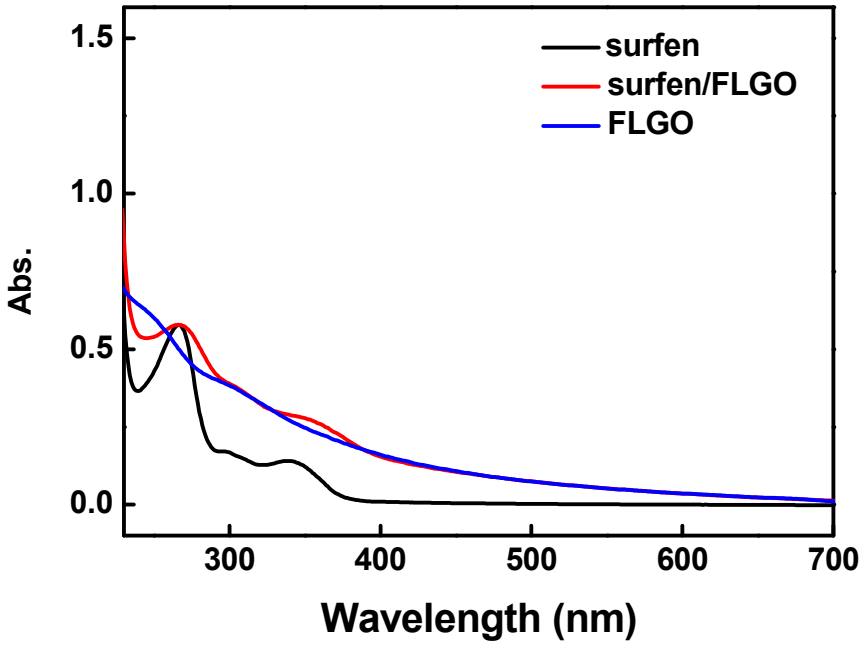

Figure S11. Absorption spectra of 10 μM surfen (black line), 15 μg/mL FLGO (blue line), and surfen-assembled FLGO (red line) in 20 mM sodium acetate (pH 10.0).

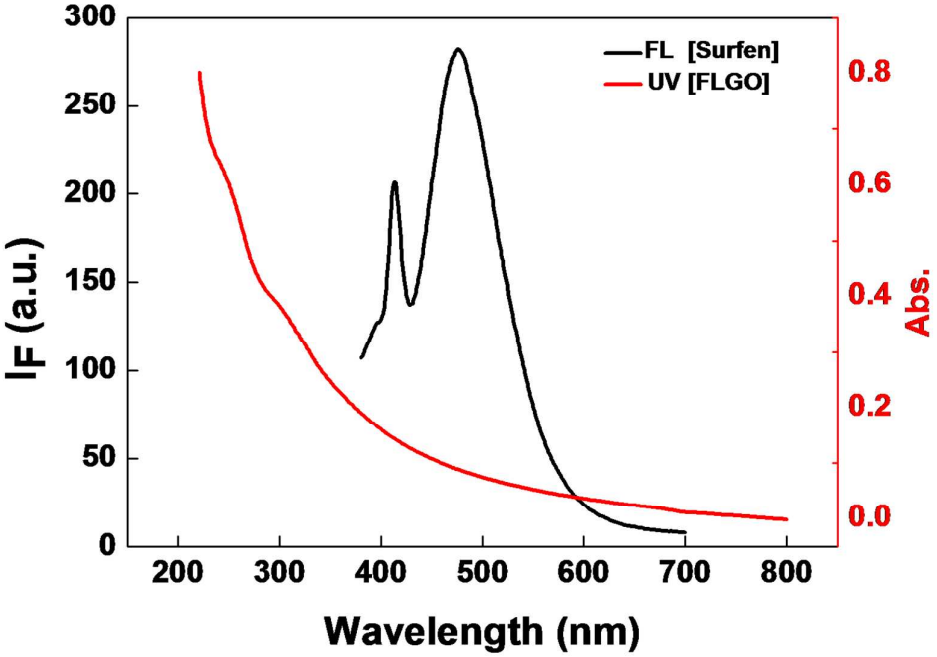

Figure S12. Fluorescence spectrum (black line) of 10 μM surfen and absorption spectrum (red line) of 15 μg/mL FLGO in 20 mM sodium acetate (pH 10.0).

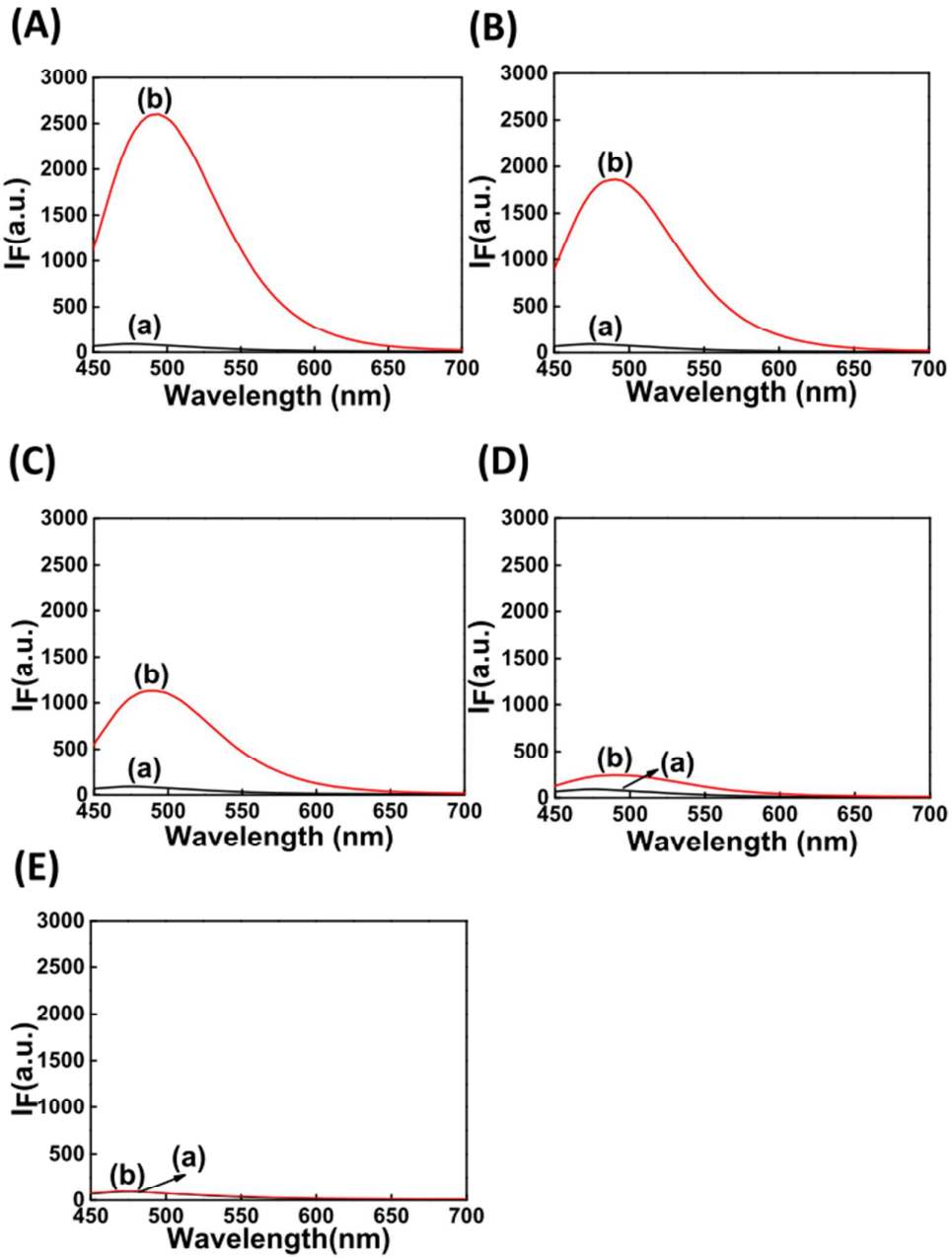

Figure S13. Fluorescence spectra of surfen-assembled FLGO (a) before and (b) after the addition of (A) OSCS, (B) heparin, (C) dermatan sulfate, (D) chondroitin sulfate A, and (E) hyaluronic acid in 20 mM sodium acetate (pH 10.0).

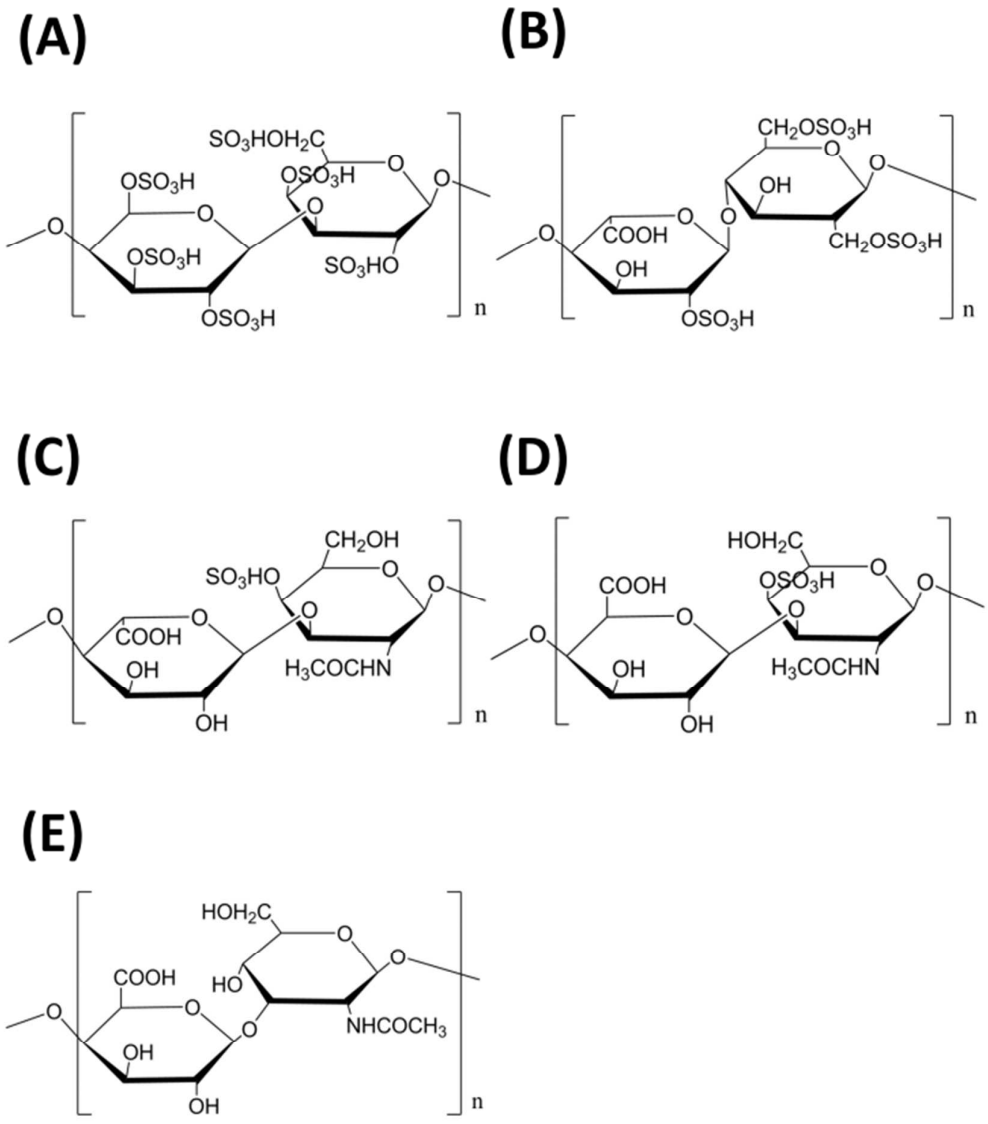

Figure S14. Chemical structures of sulfated GAGs: (A) OSCS, (B) heparin, (C) dermatan sulfate, (D) chondroitin sulfate A, and (E) hyaluronic acid.

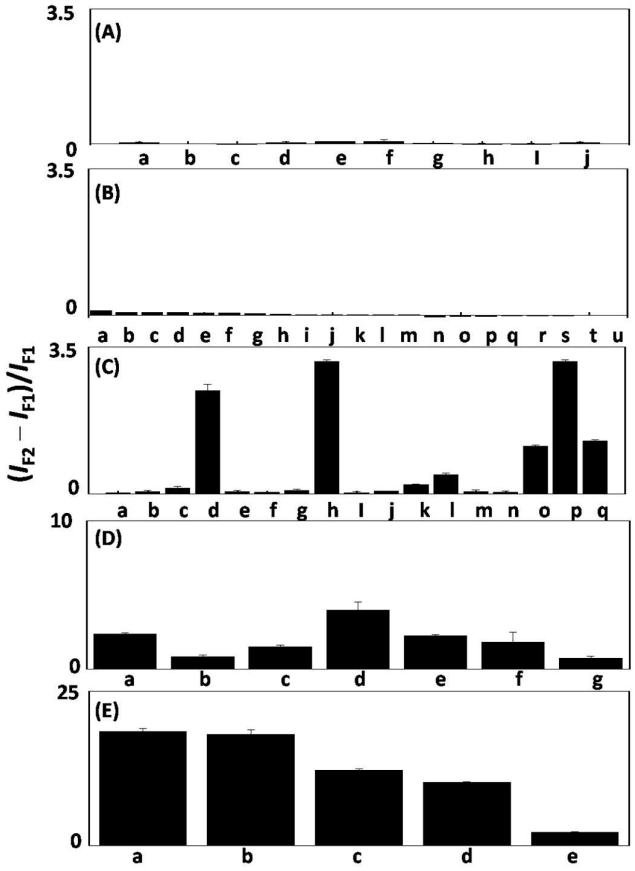

Figure S15. Relative fluorescence intensity [$(I_{F2} - I_{F1})/I_{F1}$] at 485 nm obtained from the addition of possible interfering substance to a solution of surfen at pH 10.0. (A) metal ion: (a) 2 mM Ca(II), (b) 10 μM Zn(II), (c) 10 μM Pb(II), (d) 100 mM Na(I), (e) 1 mM Mg(II), (f) 100 mM K(I), (g) 10 μM Hg(II), (h) 10 μM Fe(II), (i) 10 μM Fe(III), and (j) 10 μM Cu(II). (B) 10 μM amino acid: (a) alanine, (b) arginine, (c) asparagine, (d) aspartic acid, (e) cysteine, (f) cystine, (g) glutamine acid, (h) glutamine, (I) glycine, (j) histidine, (k) proline, (l) isoleucine, (m) leucine, (n) lysine, (o) methionine, (p) threonine, (q) tyrosine, (r) serine, (s) valine, (t) tryptohan, and (u) phenylalanine. (C) 10 μM nucleotide: (a) adenosine, (b) adenosine monophosphate, (c) adenosine diphosphate, (d) adenosine triphosphate, (e) thymidine, (f) thymidine monophosphate, (g) thymidine diphosphate, (h) thymidine triphosphate, (i) cytidine, (j) cytidine monophosphate, (k) cytidine diphosphate, (l) cytidine triphosphate, (m) guanosine, (n) guanosine monophosphate, (o) guanosine diphosphate, (p) guanosine triphosphate, and (q) 20-repeat adenosines. (D) 10 μM protein: (a) bovine serum albumin, (b) cytochrome C, (c) hemoglobin, (d) human serum albumin, (e) lysozyme, (f) myoglobin, and (e) trypsin. (E) 1 μM GAGs: (a) OSCS, (b) heparin, (c) dermatan sulfate, (d) chondroitin sulfate A, and (e) hyaluronic acid. The error bars represent standard deviations based on three independent measurements.

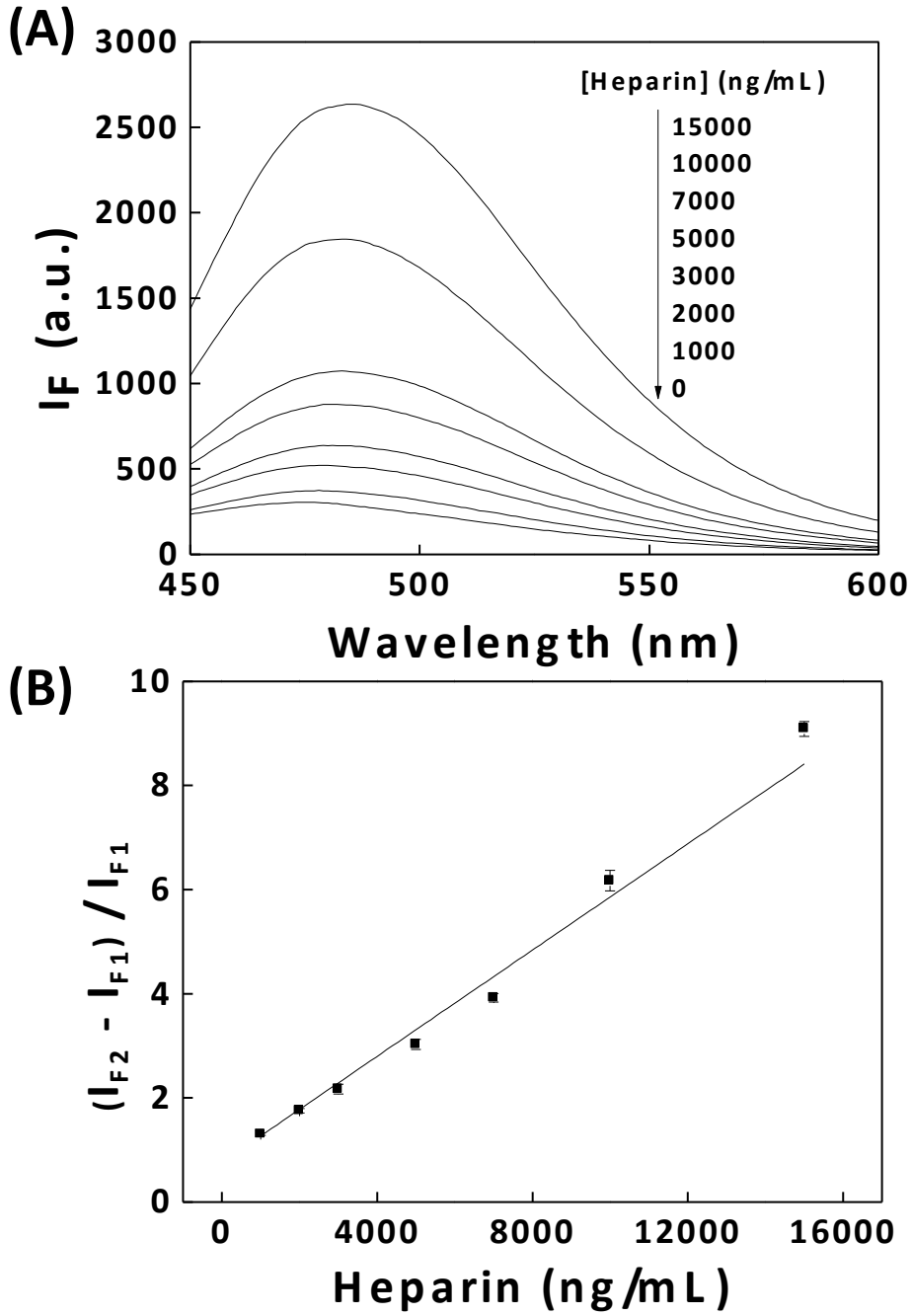

Figure S16. (A) Fluorescence spectra obtained by the addition of 0–15000 ng/mL heparin to a solution of surfen at pH 10.0. (B) A plot of the value of $(I_{F2} - I_{F1})/I_{F1}$ at 485 nm versus the concentration of heparin.

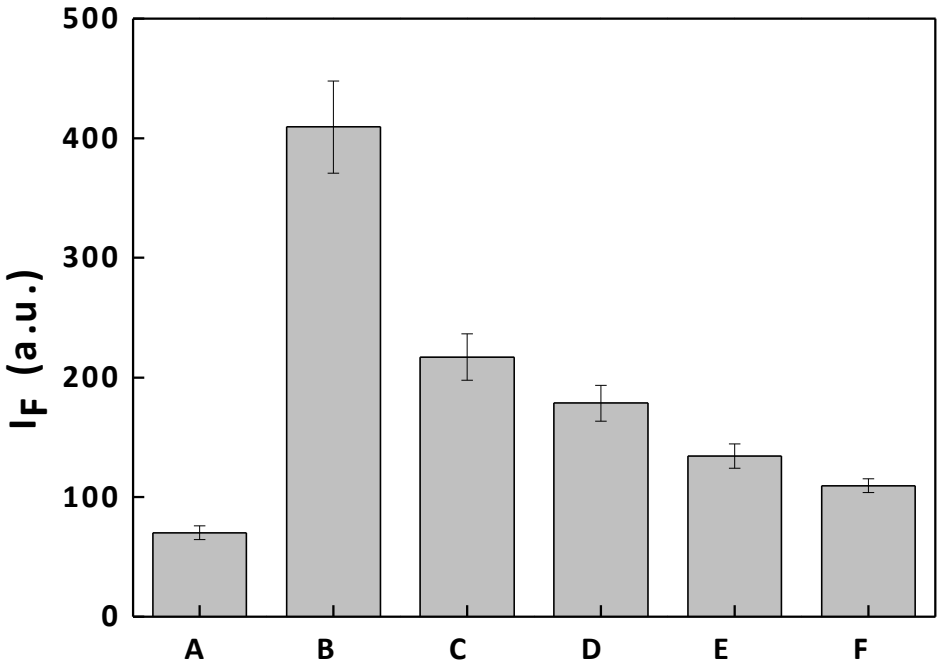

Figure S17. Fluorescence intensity obtained from the incubation of surfen-assembled FLGO in different matrices. (A) acetate-NaOH solution, (B) plasma, (C) 5-fold diluted plasma, (D) 10-fold diluted plasma, (E) 50-fold diluted plasma, and (F) 100-diluted plasma.

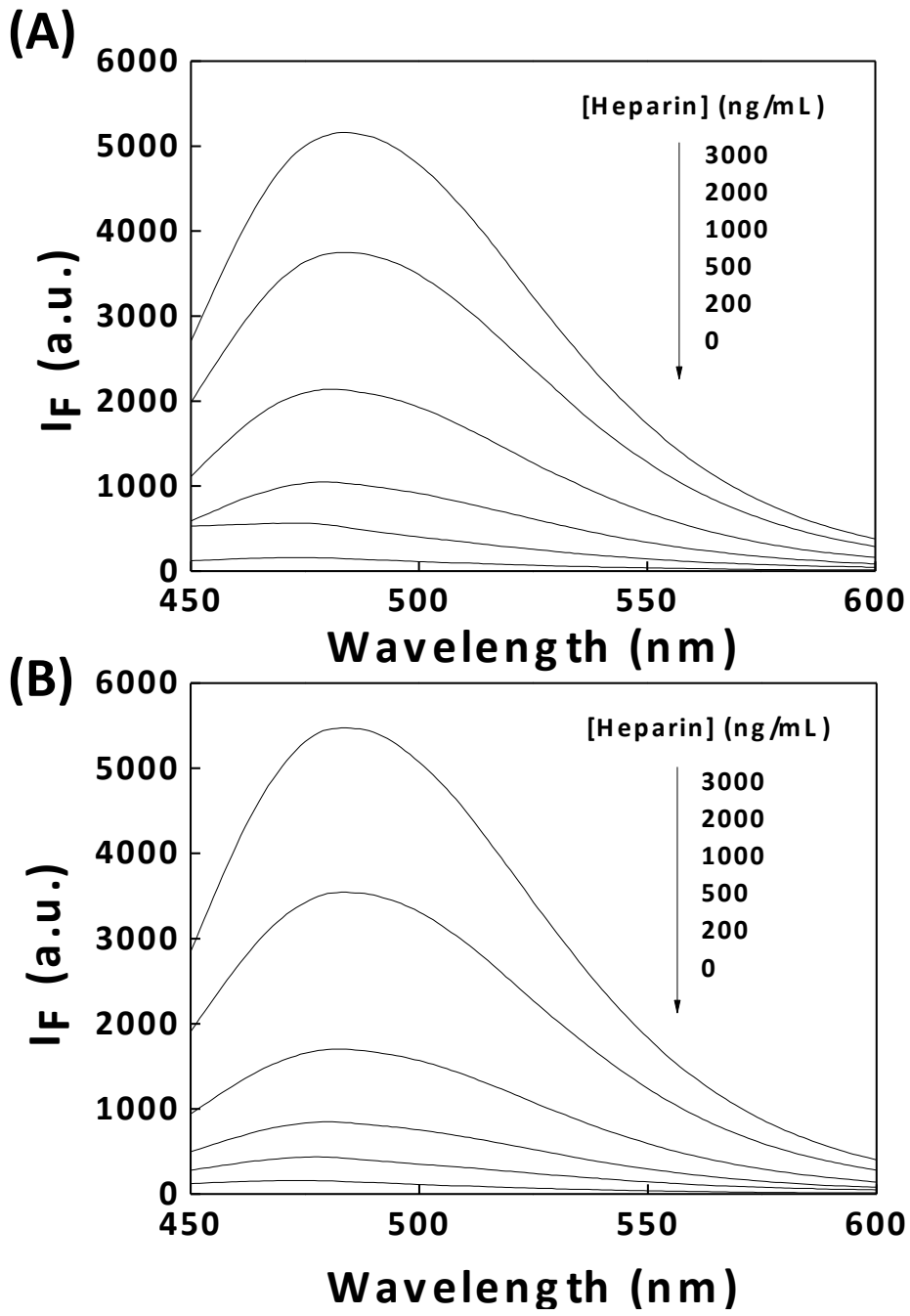

Figure S18. Fluorescence spectra obtained from the addition of heparin-spiked plasma (A) Sample 2 and (B) Sample 3 to a solution of surfen-assembled FLGO at pH 10.0. The arrow indicates the signal changes as increases in heparin concentration in plasma (A) Sample 2 and (B) Sample 3.

Table S1. Comparison of the proposed probe and the other previously reported methods for the determination of heparin.

Sensor	Detection	Linear range	Limit of detection	
Gold nanorods	Colorimetry	0.02 - 0.28 μg/mL	0.5 ng/mL	49
Positively-charged gold nanoparticles	Colorimetry	0.09 - 3.12 μg/mL	300 ng/mL	50
Adenosine-based molecular beacons	Fluorescence	0.18 - 72 μg/mL	60 ng/mL	51
Polyadenosine-coralyne complex	Fluorescence	0 – 1.8 μg/mL	75 ng/mL(4 nM)	52
Pyrene derived	Fluorescence	0 - 6.12 μg/mL	0.1224 μg/mL	53
Siole derived	Fluorescence	0-198 μg/mL	414 ng/mL	54
Diversity oriented fluorescence library approach(DOFLA)	Fluorescence	1.8 – 180 μg/mL		55
Boronic acid-containing amino acid	Colorimetric			56
Conjugated polyelectrolytes	Fluorescence	0- 1296 μg/mL		57
Cationic polythiophene	Colorimetry	0-102.51 μg/mL	15.3 μg/mL	58
Polymeric heparin sensor	Fluorescence	0.54-3.6μg/mL		59
Polyethyleneimine capped Mn-Doped ZnS Quantum Dots	Fluorescence	540-1260 μg/mL	10.44 μg/mL	60
Surfen-assembled GO	Fluorescence	3000-100 ng/mL	30 ng/mL	This study